[5] Powell, A., "On the noise emanating from a two-dimensional jet above the critical pressure," Aeronaut. Quart. IV, Part II, 103–122 (February 1953).

[6] Powell, A., "On the mechanism of choked jet noise," Proc. Phys. Soc. 866, 1039 (1953).

[7] Lam, S. H., "Interaction of two-dimensional inviscid incompressible jet facing a hypersonic stream," Princeton Univ. AFOSR-TN-59-274 Rept. 447 (March 1959).

[8] Stalder, J. R. and Inouye, M., "A method of reducing heat transfer to blunt bodies by air injection," NACA RM A56B27a (May 17, 1956).

[9] Charzenko, N. and Hennessey, K., "Investigation of a retrorocket exhausting from the nose of a blunt body into a supersonic free stream," NASA TN-D-751 (September 1961).

[10] Romeo, D. J. and Sterett, J. R., "Exploratory investigation of the effect of a forward facing jet on the bow shock of a blunt body in a Mach number 6 free stream," NASA TN D-1605 (February 1963).

[11] Dosanjh, D. S., "Experiments on interaction between a traveling shock wave and a turbulent jet," J. Aeronaut. Sci. 24, 838–844 (1957).

[12] Dosanjh, D. S., "Use of a hot wire anemometer in shock tube investigations," NACA TN 3163 (December 1954).

[13] Dosanjh, D. S. and Weeks, T. M., "Interaction of traveling shock wave with turbulent flow fields," Syracuse Univ. Final Rept. ME552-6204F; also Armed Services Tech. Info. Agency AD 275 631 (April 1962).

[14] Weeks, T. M., "Interaction of traveling shock wave with opposing axisymmetric turbulent jet," Master's Thesis, Dept. Mech. Eng., Syracuse Univ. (January 1961).

[15] Rouse, H. (ed.), *Advanced Mechanics of Fluids* (John Wiley and Sons, 1959), Chap. VIII, Sec. D.

[16] Kuethe, A. M., "Investigations of the turbulent mixing regions formed by jets," J. Appl. Mech. 2, no. 3, A 87–95 (September 1935).

[17] Lighthill, M. J., "On sound generated aerodynamically II," Proc. Roy. Soc. (London) 222A, 1–32 (1954).

JULY 1963 AIAA JOURNAL VOL. 1, NO. 7

Constant Convective Heating Rate Surfaces for Lifting Re-Entry Vehicles

WILBUR L. HANKEY JR.* AND LAWRENCE E. HOOKS†
Aeronautical Systems Division, Wright-Patterson Air Force Base, Ohio

A constant emissivity surface of known area is considered. It is assumed that heat input to the surface is balanced by radiation to space. The minimum peak temperature possible on this surface occurs when the surface temperature is constant. It is shown that constant temperature is equivalent to constant local heating rate. Constant convective heating rate contours are determined by setting Lees' 1956 equation for laminar heating rate distribution equal to unity and solving for the surfaces that satisfy that condition. The resulting nose and leading edge geometries are presented for a ratio of specific heats of 1.2. Stagnation region heating rates and temperatures for constant convective heating rate surfaces and circular arc surfaces are compared at the same flight condition. Stagnation heating rates on the constant convective heating rate surfaces are approximately 70% of the values on circular arc surfaces fitting the same vehicle.

Nomenclature

A = area
K = a constant of proportionality
n = 0 for a planar body, 1 for a body of revolution
P = local static pressure
$\overline{Pr}$ = average Prandtl number
q = local heat transfer rate per unit area
Q = total heat transfer rate
R = local radius of curvature
S = distance along body surface from stagnation point
T = absolute temperature
V = local inviscid gas velocity, tangent to the body except when freestream conditions are indicated
x = distance along body axis from stagnation point
y = distance from body axis to body surface
β = dimensionless stagnation point velocity gradient, $(1/V_\infty)$, $(dV_\delta/d\theta)_S$ equal to $\{(\gamma - 1)/\gamma\}^{1/2}$
γ = effective ratio of specific heats
ϵ = emissivity
θ = angle between tangent plane at local body point and tangent plane at the stagnation point
μ = absolute viscosity
σ = Stephan-Boltzmann constant
ω = μ/RT

Subscripts

a = conditions at point where sonic velocity occurs
c = conditions on a surface with circular arc cross section
E = conditions on a surface with an elliptical cross section
0 = condition at the termination of constant heating rate surface
S = stagnation point conditions
δ = conditions at outer edge of boundary layer
∞ = freestream conditions

Received by ARS October 11, 1962; revision received May 9, 1963.

* Chief, Aerodynamics Branch, Dyna-Soar System Program Office.

† Physicist, Aerothermodynamics Unit, Flight Dynamics Laboratory.

I. Introduction

RE-ENTRY vehicles may be classed as ballistic vehicles or lifting vehicles. Ballistic vehicles are characterized by short re-entry time and turbulent boundary layer during the critical heat pulse. Lifting vehicles have a long re-entry time and laminar boundary layer during their critical heat pulses.

The flight corridor of either type of re-entry vehicle is limited by its ability to absorb or reject the re-entry heat load. The heat pulse applied to a ballistic vehicle during re-entry is of such short duration that cooling by ablation allows the vehicle to survive. Because of long re-entry times, however, it is probable that lifting re-entry vehicles will rely on cooling by reradiation over significant portions of their flight paths.

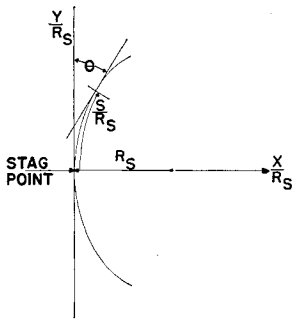

Fig. 1 Geometric relation of coordinates on constant heating rate surfaces

Cooling by reradiation appears likely especially for the long suborbital heating pulse.

When vehicle cooling is by reradiation exclusively, long re-entry times and small skin heat capacities will lead to near equilibrium between heat imposed on and heat radiated away from the surface. This equilibrium situation implies that the temperature of a radiating surface of fixed geometry must increase if the heating rate to the surface increases. This will occur on a lifting re-entry vehicle if its velocity is increased at a given altitude. Thus, the flight corridor of a lifting re-entry vehicle cooled by reradiation is limited by the maximum temperature its skin will withstand.

Consider a vehicle that has its flight corridor constrained by nose and/or leading edge temperature limits. On such a vehicle, nose and leading edge contours, which reduce surface temperatures for a given flight condition, will allow a wider vehicle flight corridor for a fixed limiting skin temperature.

A heat transfer model of the nose and leading edge regions of lifting re-entry vehicles cooled by reradiation may be developed by assuming a constant emissivity skin that maintains thermal equilibrium by radiating its total heat input to space. For this model, it will be shown that the surface of given area which minimizes peak temperature for a fixed total heating rate is one with constant local heating rate.

The conclusions just outlined show the desirability of finding constant heating rate contours for the nose and leading edges of lifting re-entry vehicles. The greatest gains from leading surface contouring will occur if those surfaces are contoured to relieve the peak heating. Since lifting re-entry vehicles have peak stagnation region heating at high altitudes, it is probable that the peak heating occurs while the boundary layers in the critical regions are laminar. Assuming this, and assuming that shock layer radiation heating is negligible suborbitally, Lees' convective heating distribution is taken to give the complete heating distribution on blunt leading edges and noses. Lees' equation is restricted so that the local heating rate is constant over the surface. This restricted equation is solved for the nose and leading edge contours that have constant convective heating rate.

Finally, the practical benefits of the constant convective heating rate surfaces are estimated by comparing their stagnation temperature and heating rates with those of circular arc leading edges and noses which fit the same vehicle.

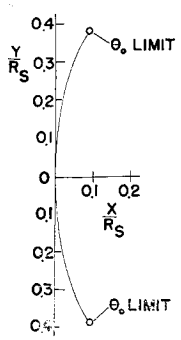

Fig. 2 Typical constant heating rate surface

II. Minimum Peak Temperature Surface

The total heating rate into a surface in radiation equilibrium may be expressed as follows:

$$Q = \int q\, dA = \epsilon\sigma \int T^4\, dA \tag{1}$$

where constant emissivity has been assumed. An average temperature may be defined as follows:

$$T_{\text{avg}}{}^4 \int dA = \int T^4\, dA \tag{2}$$

or

$$\frac{1}{A}\int \left(\frac{T}{T_{\text{avg}}}\right)^4 dA = 1 \tag{3}$$

If a region of A exists for which $T < T_{\text{avg}}$, Eq. (3) shows that another region must exist for which $T > T_{\text{avg}}$. Thus, the surface characterized by A, Q, and ϵ which has a constant surface temperature $T \equiv T_{\text{avg}}$ has the minimum peak temperature of all surfaces characterized by A, Q, and ϵ.

q is an increasing function of T, and so a constant $T \equiv T_{\text{avg}}$ implies a constant $q \equiv q_{\text{avg}}$. Therefore, for a surface characterized by A, Q, and ϵ which is maintaining thermal equilibrium by radiation, the minimum peak temperature will occur when the local heating rate on A is a constant $q \equiv \epsilon\sigma T_{\text{avg}}{}^4$. Note that T is an increasing function of q, and so $q \equiv q_{\text{avg}}$ implies $T \equiv T_{\text{avg}}$. Thus, the condition that surface temperature be constant on A is equivalent to the condition that heat transfer rate be constant on A.

III. Geometric Shapes Giving Constant Local Heating Rate over a Blunt Nose or Leading Edge

Lees[1] describes the convective heat transfer rate near the stagnation point of a blunt body in hypersonic flight by

$$\frac{q}{q_S} = \frac{F(S)}{2^{n/2}[(1/R_S)(RdV_\delta/V_\infty dS)_S]^{1/2}} \tag{4}$$

where

$$F(S) = \frac{(P/P_S)(\omega_\delta/\omega_S)(V_\delta/V_\infty)y^n}{\left[2\int_0^S \frac{P}{P_S}\frac{\omega_\delta}{\omega_S}\frac{V_\delta}{V_\infty}\, y^{2n}\, dS\right]^{1/2}} \tag{5}$$

where $n = 0$ for a planar body and $n = 1$ for a body of revolution. In developing Eq. (4) the following assumptions were made: 1) heating due to radiation from the shock layer may be neglected; 2) the boundary layer and shock wave are distinct; and 3) the pressure gradient a tthe surface is negligible at hypersonic speeds so that the enthalpy gradient there is given by $0.47\ (\overline{Pr})^{1/3}$, and the surface heat transfer rate distribution is obtained directly from the surface pressure distribution.

The static pressure ratio will be represented by the Newtonian flow approximation

$$P/P_S = \cos^2\theta \tag{6}$$

with θ defined in Fig. 1. Measurements by Creager[2] and others show that the total pressure is nearly constant along inviscid streamlines following a blunt body contour. Assuming this, the local velocity at the outer edge of the boundary layer may be related to the local pressure by the following isentropic relationship:

$$(V_\delta/V_\infty)^2 = (2h_s/V_\infty{}^2)\{1 - (P/P_s)^{(\gamma-1)/\gamma}\} \tag{7}$$

For hypersonic velocities

$$2h_s/V_\infty{}^2 \approx 1 \tag{8}$$

Substituting Eqs. (6) and (8) in Eq. (7) gives

$$V_\delta/V_\infty = [1 - \cos^{2\beta^2}\theta]^{1/2} \tag{9}$$

Table 1 Coordinates of the constant heating rate surface ($\gamma = 1.2$, $\beta = 0.40825$)

	$n = 0$			$n = 1$		
θ, deg	$\frac{x}{R_s}$	$\frac{y}{R_s}$	$\frac{1}{R_s}\frac{dS}{d\theta}$	$\frac{x}{R_s}$	$\frac{y}{R_s}$	$\frac{1}{R_s}\frac{dS}{d\theta}$
0	0	0	1.00000	0	0	1.00000
2	0.60796^{-3}	0.34726^{-1}	0.99654	0.60800^{-3}	0.34855^{-1}	0.99619
4	0.24187^{-2}	0.69298^{-1}	0.98623	0.24174^{-2}	0.69403^{-1}	0.98482
6	0.53919^{-2}	0.10330	0.96930	0.53847^{-2}	0.10334	0.96598
8	0.94610^{-2}	0.13646	0.94622	0.94382^{-2}	0.13638	0.93986
10	0.14534^{-1}	0.16851	0.91800	0.14479^{-1}	0.16823	0.90672
12	0.20497^{-1}	0.19921	0.88174	0.20385^{-1}	0.19863	0.86689
14	0.27212^{-1}	0.22831	0.83937	0.27010^{-1}	0.22735	0.82076
16	0.34522^{-1}	0.25561	0.79125	0.34190^{-1}	0.25416	0.76881
18	0.42254^{-1}	0.28092	0.73773	0.41742^{-1}	0.27888	0.71156
20	0.50220^{-1}	0.30408	0.67923	0.49474^{-1}	0.30136	0.64960
22	0.58222^{-1}	0.32494	0.61622	0.57185^{-1}	0.32147	0.58361
24	0.66053^{-1}	0.34341	0.54919	0.64668^{-1}	0.33911	0.51429
26	0.73501^{-1}	0.35940	0.47866	0.71721^{-1}	0.35425	0.44240
28	0.80355^{-1}	0.37286	0.40519	0.78143^{-1}	0.36688	0.36876
30	0.86406^{-1}	0.38380	0.32939	0.83746^{-1}	0.37700	0.29422
32	0.91451^{-1}	0.39221	0.25185	0.88358^{-1}	0.38469	0.21964
34	0.95299^{-1}	0.39815	0.17320	0.91824^{-1}	0.39004	0.14594
36	0.97770^{-1}	0.40169	0.94108^{-1}	0.94016^{-1}	0.39318	0.73984^{-1}
38	0.98704^{-1}	0.40294	0.10310^{-1}	0.94831^{-1}	0.39428	0.46659^{-2}

where $\beta^2 = (\gamma - 1)/\gamma$. The velocity gradient may now be determined:

$$dV_\delta/dS = V_\infty\beta^2\,[1 - \cos^{2\beta^2}\theta]^{-1/2}\cos^{2\beta^2}\theta\,\tan\theta(d\theta/dS) \quad (10)$$

The value of the velocity gradient at the stagnation point is required for Lees' heating rate equation:

$$\left(\frac{R}{V_\infty}\frac{dV_\delta}{dS}\right)_s = \left[\frac{\beta^2\tan\theta}{(1 - \cos^{2\beta^2}\theta)^{1/2}}\right]_{\theta\to 0} = \beta \quad (11)$$

where $R = dS/d\theta$. By using Eqs. (5, 6, 9, and 11) in Eq. (4) the heating rate distribution may be obtained for an arbitrary body. Following Lees,[1] the assumption is made that $\omega_\delta/\omega_S = 1$ in hypersonic flight:

$$\frac{q}{q_s} = \frac{\cos^2\theta(1 - \cos^{2\beta^2}\theta)^{1/2}(y/R_s)^n}{2^{(n+1)/2}\beta^{1/2}\left[\int_0^{S/R_s}\cos^2\theta(1 - \cos^{2\beta^2}\theta)^{1/2}\left(\frac{y}{R_s}\right)^{2n}d\left(\frac{S}{R_s}\right)\right]^{1/2}} \quad (12)$$

Wagner, Pine, and Henderson[3] have shown experimentally that Lees' equation in the forementioned form holds well for a series of blunt-nosed bodies with noncircular cross sections. The noses of these bodies are described by $x = Ky^m$, where x is the axial distance from the stagnation point and y is perpendicular to x. Blunt bodies were tested with $m = 2, 4, 6, 8$; and a hemisphere-cylinder was tested for comparison.

Since R_s appears only as a scaling factor in Eq. (12), it may be assumed to be unity without loss of generality. To have a constant heating rate over the surface, the heating rate ratio of Eq. (12) must be unity. Defining

$$g(\theta) = \cos^2\theta(1 - \cos^{2\beta^2}\theta)^{1/2} \quad (13)$$

the equation for a constant heating rate surface becomes (after squaring)

$$\beta 2^{n+1}\int_0^S y^{2n}\,g(\theta)\,dS = g^2(\theta)y^{2n} \quad (14)$$

The geometric relationships of x, y, S, θ are as follows (see (Fig. 1):

$$dx/d\theta = \sin\theta(dS/d\theta) \quad (15)$$

$$dy/d\theta = \cos\theta(dS/d\theta) \quad (16)$$

and

$$dS/d\theta = [(dg/d\theta)/\{\beta 2^n - (ng/y)\cos\theta\}] \quad (17)$$

obtained by differentiating Eq. (14).

Numerical solutions were obtained for two- and three-dimensional cases ($n = 0$ and 1, respectively) and for values of γ of 1.2, 1.4, and 1.6, by simultaneous integration of Eqs. (15–17) with the initial boundary conditions that $x = 0$, $y = 0$ at $\theta = 0$. Numerical results for $\gamma = 1.2$ are given in Table 1. Figure 2 shows a cross section of the constant heating rate surface with $n = 1$, $\gamma = 1.6$. The constant heating rate surfaces are so similar that x/R_s varies less than 3% for the six cases at a y/R_s of 0.394, a value near the maximum y/R_s. Thus, Fig. 2 is representative of all six cases.

The heating rate distributions over two- and three-dimensional elliptical surfaces have been computed using an equation identical to Eq. (12). Surfaces, formed from an ellipse with a major to minor axis ratio of two, have heating rate distributions that are within 3% of the stagnation value for $0° \leq \theta \leq 30°$ when the minor axis is parallel to the free-stream velocity vector. This condition was found to hold for $n = 0$, 1 and $1.2 \leq \gamma \leq 1.6$.

IV. Limit of the Constant Local Heating Rate Surface

Inspection of Eq. (17) shows that $dS/d\theta$ is a monotonic-decreasing function of θ. This means that a continuously decreasing local radius of curvature is necessary to maintain heating rate constant as θ increases away from the stagnation point. The numerator becomes zero when

$$(2 + \beta^2)\cos^{2\beta^2}\theta - 2 = 0 \text{ for } 0° < \theta < 90° \quad (18)$$

Solving for θ,

$$\theta_0 = \cos^{-1}[2/(3\gamma - 1)]^{\gamma/2(\gamma-1)} \quad (19)$$

At this angle, a cusp occurs in the constant heating rate surface. Therefore, beyond θ_0, it is not possible to maintain a constant heating rate distribution on a smoothly curved surface suitable for vehicle application. For practical construction, the radius at any $\theta < \theta_0$ may be continued in a circular arc to the aft wing or body surfaces. Since the circular arc has a constant radius, whereas a decreasing one is necessary for constant heating rate, the actual heating rate will fall off smoothly past the point chosen to begin the circular arc.

This simple method retains the value of the constant heating rate surface, as no temperature increase is experienced

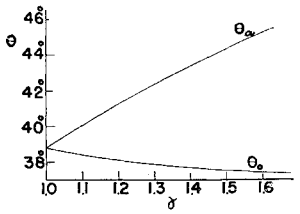

Fig. 3 Angular location of sonic line, θ_a, and limiting line for constant heating rate surface, θ_0, vs γ, effective ratio of specific heats

passing from the constant heating rate surface to the upper and lower wing surface. Any surface with a local radius of curvature at least equal to that of the constant heating rate surface may be used to complete the leading edge without causing a temperature increase if the two surfaces are matched smoothly.

V. Sonic Line on the Leading Edge and Nose Surface

Bernoulli's equation for the pressure ratio of an isentropic, perfect, compressible gas is

$$P/P_s = \{1 + [(\gamma - 1)/2]M\}^{-[\gamma/(\gamma-1)]} \tag{20}$$

Combining Eqs. (20) and (6) for $M = 1$,

$$\theta_a = \cos^{-1}\{2/(\gamma + 1)\}^{\gamma/2(\gamma+1)} \tag{21}$$

Figure 3 shows θ_0, the limiting value of the constant heating rate surface, and θ_a, the angle at which sonic velocity occurs, as a function of γ. This figure shows that a constant heating rate may be maintained only in the subsonic flow region of a surface. As γ goes to 1, both θ_0 and θ_a converge to 38.850°.

VI. Reduction in Stagnation Heating Rate and Temperature Gained from Constant Heating Rate Surfaces

It has been shown that constant heating rate surfaces have the minimum peak temperatures possible to surfaces of constant emissivity, area, and total heat input rate. To evaluate the practical gains due to a constant heating rate surface, its stagnation heating rate and temperature must be compared to other leading edge and nose surfaces sized to fit the same vehicle. This comparison must assume one flight condition for both surfaces. These surfaces cannot be compared directly by the technique of Sec. II, since both surface area and total heat input rate vary for a series of leading edges or noses fitting a given vehicle at a given point on its flight profile.

Two cases are compared here. First, the constant heating rate nose for $\gamma = 1.2$ is compared to a hemisphere nose. No allowance is made for matching the constant heating rate nose to the body with circular arc extensions, and so this is a limiting case. Second, the 2 to 1 ellipse, which approximates a constant heating rate surface with its smooth matching surface, is compared to a surface with a circular arc cross section.

From Table 1, the limiting y/R_s value for the $\gamma = 1.2$ constant heating rate nose is $y/R_s = 0.39428$. y is the distance from the axis of symmetry to the surface, and so it corresponds to the radius of the hemisphere nose. Thus

$$q_s/q_{sc} = (y/R_s)^{1/2} = 0.628 \tag{22}$$

when the flight condition is the same for both surfaces. Assuming that the temperatures are related to the heat fluxes by the Stefan-Boltzman law,

$$T_s/T_{sc} = 0.89 \tag{23}$$

To compare a surface having a 2 to 1 ellipse for a cross section with one having a circular arc cross section, equate the length of the major axis to the length of the circle diameter. Assuming that the minor axis of the ellipse is parallel to the freestream velocity vector, the radius of curvature of the ellipse at the geometric stagnation point is

$$R_{SE} = R_{sc}^2/(R_{sc}/2)$$

and so

$$q_{SE}/q_{sc} = 0.7071 \tag{24}$$

when the two surfaces are at the same flight condition. Assuming that the surfaces are radiation cooled and in equilibrium with the convective heat flux,

$$T_{SE}/T_{sc} = 0.917 \tag{25}$$

These figures apply to leading edges and noses both, since the variation of stagnation heating rate with radius of curvature is the same for both at a fixed flight condition.

These two computations demonstrate that constant heating rate noses and leading edges will reduce substantially the stagnation heating rates and temperatures when these surfaces replace circular arc surfaces on radiation-cooled lifting re-entry vehicles with negligible heating due to shock layer radiation. The exact gains obtained from the constant heating rate surfaces depend on the surface orientation on the vehicle and the technique used to match the surface to the vehicle.

VII. Conclusions

It was shown that a constant temperature over a constant emissivity surface is the minimum peak temperature possible for a given average heating rate when the surface is cooled by radiation alone. A constant temperature surface was shown to be equivalent to a constant heating rate surface. Two- and three-dimensional constant heating rate surfaces were developed for vehicle leading surfaces covered by laminar boundary layers and heated by convection only. Variation of the x/R_s and y/R_s coordinates of the constant heating rate surfaces are 4% and 2%, respectively, when two- and three-dimensional cases are compared separately for $1.2 \leq \gamma \leq 1.6$ at $\theta = 36°$. The maximum variation of each coordinate is 8% and 4%, respectively, at $\theta = 36°$ for $n = 0$ and 1 and $1.2 \leq \gamma \leq 1.6$.

The constant heating rate condition may be maintained only in the subsonic flow field. The laminar heating rate on a smooth body will diminish always as the flow goes supersonic.

It was stated that the blunter side of a 2 to 1 ellipse would maintain a heating rate over its surface which varied only $\pm 3\%$ from a constant value out to $\theta = 30°$.

The constant heating rate nose for $\gamma = 1.2$ was compared to a hemisphere fitting the same vehicle. The stagnation heating rates and temperatures were compared for those surfaces, and the 2 to 1 elliptical surface was compared to a circular arc surface. This second comparison was valid for both two- and three-dimensional situations. Both cases showed the heating rate on the blunt surfaces to be about 70% that of the circular arc surface. The corresponding temperatures were shown to be about 90% of those on the circular arc surfaces.

The family of constant heating rate surfaces was developed theoretically to be minimum temperature surfaces. Computations based on different, practical assumptions showed that these surfaces significantly reduce stagnation temperature compared to circular arc surfaces.

References

[1] Lees, L., "Laminar heat transfer over blunt nosed bodies at hypersonic flight speeds," Jet Propulsion **26**, 259 (April 1956).

[2] Creager, M. O., "Effects of leading-edge blunting on the local heat transfer and pressure distributions over flat plates in supersonic flow," NASA TN 4142 (1957).

[3] Wagner, R., Pine, W., and Henderson, A., "Laminar heat-transfer and pressure-distribution studies on a series of re-entry nose shapes at a Mach number of 19.4 in helium," NASA TN D-891 (June 1961).